Reversal of the parallel drift frequency in anomalous transport of impurity ions

Shaokang Xu[1,2], S. Maeyama[1,3], T.-H. Watanabe[1] and Ö. D. Gürcan[4]
[1]*Nagoya University, Furo-cho, Nagoya 464-8602 Japan*
[2]*Southwestern Institute of Physics, P.O. Box 432, Chengdu 610041, People's Republic of China*
[3]*National Institute for Fusion Science, Toki,Gifu 509-5292, Japan*
[4]*Laboratoire de Physique des Plasmas, CNRS, Ecole Polytechnique, Sorbonne Université, Université Paris-Saclay, Observatoire de Paris, F-91120 Palaiseau, France*

We study the heavy ion transport with the gyrokinetic simulation and find that when the gradient of the turbulence intensity is enhanced along the magnetic field line, part of the particles in velocity space reverses the parallel drift frequency. As a result, the particle transport related to the parallel dynamics is strongly enhanced. The parallel drift frequency is derived and shows that the frequency reversal is due to the amplitude effect of the turbulence on the plasma parallel structure and occurs when the gradient of turbulence intensity becomes large along the magnetic field line.

Introduction.–Turbulence in space and laboratory plasmas have extensively been studied in the past by focusing on phenomena that are perpendicular to the magnetic field lines, as in the case of ion temperature gradient driven, or trapped electron mode turbulence[1–7], while the turbulent dynamics parallel to the magnetic field lines are averaged out on the magnetic surface as is commonly done in data analysis or resolved using an approximate method as in most analytical calculations. For example, in many theoretical studies of plasma turbulence, to simplify the notation of the parallel dynamics, it is conventional to replace the parallel advection $v_\parallel \nabla_\parallel$ by $ik_\parallel v_\parallel$, with $k_\parallel$, a parallel wavenumber[8–13]. This insinuates that the particles with positive and negative parallel velocities along the magnetic field lines also have opposite parallel frequencies, and since the particle transport related to the parallel dynamics is proportional to this parallel frequency, the contribution from particles with $v_\parallel > 0$ are canceled or at least significantly reduced by the contribution from the particles with $v_\parallel < 0$.

In this work we study the heavy ion transport with the gyrokinetic simulations using the GKV Code[14]. We show that the conventional solution is actually the phase effect of the turbulence on the ion parallel structure and works when the gradient of the turbulence intensity is weak along the magnetic field line. However, when the gradient of the turbulence intensity is enhanced, for example using a strong magnetic shear or a large safety factor, the amplitude effect of the turbulence appears in the plasma parallel structure, causing a fraction of particles in velocity space reversing the sign of their parallel drift, e.g., particles with positive and negative parallel velocities may have parallel frequencies of the same sign, which differs from the conventional description. As a result, the particle transport related to the parallel dynamics is strongly enhanced. This is significant since it may totally modify the understanding of the parallel dynamics in the edge region of a fusion reactor where the magnetic shear and the safety factor are large, or in a reversed shear configuration[15–17]. It is also likely to have influences in various plasmas as the turbulence profile along the magnetic field line can be modified by various parameters. Note that the reversal of the parallel drift frequency is a novel phenomenon in kinetic plasma turbulence.

Model.–We study the plasma turbulent transport in the gyrokinetic framework. The equation is written in $(\boldsymbol{R}, E, \mu)$ coordinates, where $\boldsymbol{R}$ is the guiding center position of a particle, $E = \frac{1}{2}mv^2$is the kinetic energy, and $\mu = mv_\perp^2/2B$ is the magnetic moment defined with the particle mass m, the perpendicular velocity $v_\perp$ and the magnetic field intensity B. The electrostatic gyrokinetic Vlasov equation is written as follows[18, 19],

$$\frac{\partial g_s}{\partial t} + v_\parallel \nabla_\parallel g_s + \boldsymbol{v}_{sd}\cdot\nabla g_s + \boldsymbol{v}_{sE}\cdot\nabla g_s = \frac{e_s F_{s,M}}{T_s}\frac{\partial \langle\phi\rangle_s}{\partial t} + \boldsymbol{v}_{s*}\cdot\nabla\langle\phi\rangle_s \frac{e_s F_{s,M}}{T_s}, \quad (1)$$

where g_s and ϕ are, respectively, the non-adiabatic part of the perturbed gyrocenter distribution function and the perturbed electrostatic potential. e_s, T_s and $F_{s,M}$ are the charge, the temperature and the local Maxwellian equilibrium distribution function of the species s, and $\langle\cdot\rangle_s$ means the gyrophase-average, introducing the Bessel function J_{0s} in Fourier space. $v_\parallel$ is the velocity parallel to the magnetic field line, $\boldsymbol{v}_{sd}$, $\boldsymbol{v}_{sE}$ and $\boldsymbol{v}_{s*}$ denote the magnetic drift velocity, the $E\times B$ drift velocity and the diamagnetic drift velocity respectively, defined as $\boldsymbol{v}_{sd} \equiv \frac{\boldsymbol{b}}{e_s B}\times\left(\mu\nabla B + m_s v_\parallel^2 \boldsymbol{b}\cdot\nabla\boldsymbol{b}\right)$, $\boldsymbol{v}_{sE} \equiv \boldsymbol{b}\times\frac{\nabla\langle\phi\rangle_s}{B}$, $\boldsymbol{v}_{s*} \equiv \frac{T_s\boldsymbol{b}}{e_s B}\times\left[\nabla\ln n_s + \left(\epsilon/T_s - \frac{3}{2}\right)\nabla\ln T_s\right]$, where $\boldsymbol{b}$ is the unit vector parallel to the magnetic field line. From Eq. (1), we find the particle flux related to the perpendicular and the parallel compressibility pinch as follows[20]:

$$\Gamma_s = -\frac{k_y\phi^2_{\boldsymbol{k}_\perp}}{T_s B_0}\int d^3v J_{0s}^2 e_s F_{sM} \times\frac{\left(\gamma\omega_{sd} + \gamma\kappa_r v_\parallel - \omega_r\kappa_i v_\parallel\right)}{\left(\omega_r - \kappa_r v_\parallel - \omega_{sd}\right)^2 + \left(\gamma - \kappa_i v_\parallel\right)^2}, \quad (2)$$

where ω_r is the real frequency and γ is the growth rate of the plasma turbulence. $\omega_{sd}\left(\equiv \boldsymbol{k}_\perp \cdot \boldsymbol{v}_{sd}\right)$ is the magnetic drift frequency. The first term in the numerator denotes the particle pinch (noted as $\Gamma_{s,\perp}$) caused by the perpendicular compression (due to the curvature and the gradient of the magnetic field). The second and the third terms represent the particle pinch related to the parallel dynamics (noted as $\Gamma_{s,\parallel}$), where the second term provides the effective contribution, and the third term causes the anisotropy of the particle flux on the magnetic surface and vanishes after the flux surface average[20].

Note that the conventional solution with $v_\parallel \nabla_\parallel$ replaced by $ik_\parallel v_\parallel$ is obtained with the Fourier transform, which is not problematic for a fluid quantity, such as the density. Since Fourier transform allows to well describe its parallel structure. If a principle $k_\parallel$ is not sufficient, higher order harmonic may also be involved. In this way, one always finds that for a given $k_\parallel$, particles with positive and negative parallel velocity take opposite parallel frequencies and contributes in opposite signs to the flux, resulting in the flux from one sign roughly canceling, or at least significantly reducing the flux from the other. However a kinetic quantity like the plasma distribution function depends both on the spatial and the velocity coordinates. Sustained in a turbulent electromagnetic field, particles are kicked by various forces and the parallel structure can be very complicated. In general we should have $k_\parallel = k_\parallel\left(\boldsymbol{R}, E, \mu\right)$. In order to accurately resolve the parallel structure of a kinetic plasma, we define a parallel advection operator as $i\kappa \equiv \nabla_\parallel \ln\left(g_{s\boldsymbol{k}_\perp}\right)$. If a quantity satisfies $n\left(z\right) = n_0\left(z_0\right) exp^{ik_\parallel z}$, with z, the field line coordinates, $\nabla_\parallel \ln\left(n\left(z\right)\right)$ gives nothing but a parallel wavenumber $ik_\parallel$. It is noteworthy that κ is complex, i.e., $\kappa = \kappa_r + i\kappa_i$, and based on the dimension in Eq.(2), $\kappa_r v_\parallel$ is the parallel frequency. In the next we show that the conventional solution roughly works when the gradient of the turbulence intensity is weak along the magnetic field line. In contrast however, when the gradient of turbulence intensity is enhanced, the conventional picture does not work and we need to consider the amplitude effect of the turbulence on the ion parallel structure.

Simulation results.–The simulations are performed for a toroidal plasma in the standard $\hat{s} - \alpha$ geometry. The numerical parameters employed in simulation are as follows: the electron and deuterium density and temperature gradients $R/L_{n,e} = R/L_{n,D} = 2.5$, $R/L_{T,e} = 8.0$, $R/L_{T,D} = 2.0$, respectively, the temperature $T_e = 3T_D$, the inverse aspect ratio $\epsilon = r/R = 0.105$, the safety factor $q = 1.29$ and a realistic electron to deuterium mass ratio $m_e/m_D = 1/3672$. These parameters are similar to a previous study of ASDEX-U H-mode plasma[21]. The magnetic shear $\hat{s}$ is scanned in the interval $[-1.0, 1.3]$. All these cases result in a background turbulence of trapped electron mode(TEM). Three different heavy ions: carbon $C\left(m_s = 12, e_s = 6+\right)$, iron $Fe\left(54, 20+\right)$ and tungsten $W\left(184, 40+\right)$ are also included in the simulations,

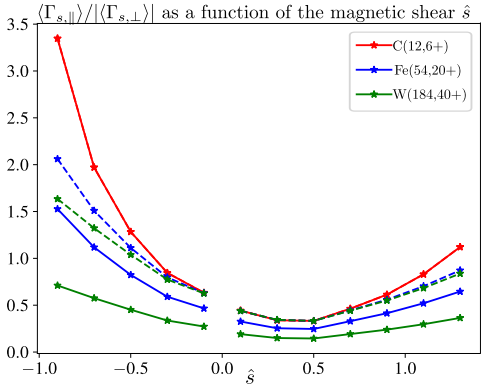

Figure 1. $\left\langle\Gamma_{s,\parallel}\right\rangle / \left|\left\langle\Gamma_{s,\perp}\right\rangle\right|$(Solid) as a function of the magnetic shear $\hat{s}$ for carbon $C\left(12, 6+\right)$ (red), iron $Fe\left(54, 20+\right)$ (blue) and tungsten $W\left(184, 40+\right)$ (green) ions. Dashed curves the normalized data by multiplying $\left(m_s/m_D\right)/e_s$ in $\Gamma_{s,\parallel}$, with $m_D = 2$, the mass of deuterium ions.

with a charge fraction of 10^{-4}[22]. Using the simulation data, $\Gamma_{s,\parallel}$ and $\Gamma_{s,\perp}$ are computed. Fig.1 shows $\left\langle\Gamma_{s,\parallel}\right\rangle / \left|\left\langle\Gamma_{s,\perp}\right\rangle\right|$as a function of the magnetic shear $\hat{s}$, where $\langle f\rangle$ means the flux surface average of f defined as $\langle f\rangle = \int \sqrt{g} f dz / \int \sqrt{g} dz$, with the Jacobian $\sqrt{g}$.

When the magnetic shear is weak, i.e., $-0.1 \leq \hat{s} \leq 0.5$, the parallel compressibility pinch $\Gamma_{s,\parallel}$ is weak in comparison to the perpendicular compressibility pinch $\Gamma_{s,\perp}$, and the difference in the particle flux of different ions are due to the mass and the charge. Therefore, we also show the normalized fluxes multiplied by $\left(m_s/m_D\right)/e_s$ in order to eliminate the e_s/m_s dependence in $\Gamma_{s,\parallel}$ [9–11, 20] in the form of dashed curves in Fig. 1, so that different ions can be compared. The profile of $\Gamma_{s,\parallel}$ and $\Gamma_{s,\perp}$ along the magnetic field line for carbon and tungsten ions are very similar in Fig. 2a with $\hat{s} = 0.3$.

However, when the magnetic shear is strong, i.e., $\hat{s} > 0.5$ or $\hat{s} < -0.1$, $\Gamma_{s,\parallel}$ is strongly enhanced in the transport of carbon and iron, while for tungsten, $\Gamma_{s,\parallel}$ increases slowly, but with a clear tendency. In the cases with a strong magnetic shear, the difference in the particle fluxes $\Gamma_{s,\parallel}$ of different ions is not simply caused by the e_s/m_s dependence, since the dashed curves in Fig. 1 are different from each other. In particular, with very strong $\hat{s}$, such as $\hat{s} = -0.7$ and $\hat{s} = -0.9$, the normalized flux of carbon is more than twice of tungsten normalized flux, hence there must be some unknown mechanisms which drive the strong transport.

As $\Gamma_{s,\parallel}$ of heavy ions like carbon is strongly enhanced compared to that of tungsten when the magnetic shear is strong, we check $\Gamma_{s,\parallel}$ and $\Gamma_{s,\perp}$ of carbon and tungsten along the magnetic field line in the simulation with a strong magnetic shear. The results with $\hat{s} = -0.9$ is shown in Fig. 2b, where the e_s/m_s dependence is removed in $\Gamma_{s,\parallel}$. In contrast to the case with $\hat{s} = 0.3$, $\Gamma_{s,\parallel}$ of carbon ions (blue solid) is strongly enhanced in high z

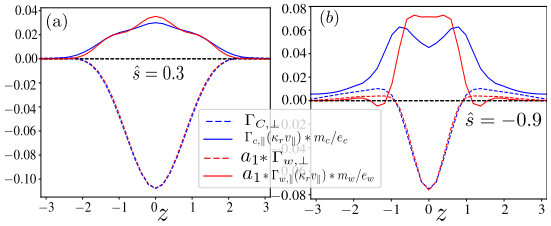

Figure 2. $\Gamma_{s,\parallel}$ (solid) and $\Gamma_{s,\perp}$ (dashed) of carbon (blue) and tungsten (red) ions as a function of the magnetic field line coordinates z in the simulations with $\hat{s} = 0.3$ (left) and $\hat{s} = -0.9$ (right). $(m_s/m_D)/e_s$ is multiplied in $\Gamma_{s,\parallel}$ to eliminate the e_s/m_s dependence.

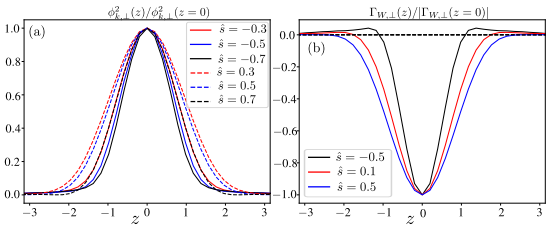

Figure 3. $\phi^2_{k_\perp}/\phi^2_{k_\perp}(z=0)$ (left) and $\Gamma_{W,\perp}/\Gamma_{W,\perp}(z=0)$ (right) as a function of z in the simulations with different magnetic shear $\hat{s}$. $z = 0$ corresponds to the outer middle plane in a tokamak configuration. Results are shown for the most unstable mode of $k_y\rho_D = 0.3$ in all these cases.

regions, compared to that of tungsten (red solid).

From Eq.(2), $\Gamma_{s,\parallel}$ is proportional to the parallel advection operator κ, which actually represents the gradient $(\nabla_\parallel)$ of the turbulence along the magnetic field line. Qualitatively, one may expect that a large gradient of the turbulence in the parallel direction results in a strong parallel compressibility pinch. The profile of the squared electrostatic potential $\phi^2_{k_\perp}$ along the magnetic field line is shown in Fig. 3a, where $\phi^2_{k_\perp}$ is normalized by its value at the outer middle plane. It shows that the gradient of turbulence intensity is enhanced with increasing the strength of magnetic shear. Hence there is a clear correlation between $\Gamma_{s,\parallel}$ and the parallel gradient of the turbulence intensity.

On the other hand, $\Gamma_{s,\perp}$ reverses its sign along the magnetic field line due to the magnetic shear, since $\Gamma_{s,\perp} \propto \boldsymbol{v}_{sd}$, which reverses the sign along the magnetic field line. In ballooning turbulence, such as ITG and TEM modes, the fluctuations are very strong on the low field side, where $\Gamma_{s,\perp}$ is directed inward (negative) and dominant. Hence $\Gamma_{s,\perp}$ is usually directed inward in both ITG and TEM turbulence[9, 10, 23]. We notice that a previous fluid simulation reports that $\Gamma_{s,\perp}$ changes from inward to outward with a negative magnetic shear [11], but it is not hard to occur in gyrokinetic turbulence due to the ballooning structure. By decreasing $\hat{s}$, the inward transport region of $\Gamma_{s,\perp}$ is decreased, as shown in Fig.3b. As a result, when $\hat{s} > 0$, both the normalized $\Gamma_{s,\parallel}$ and

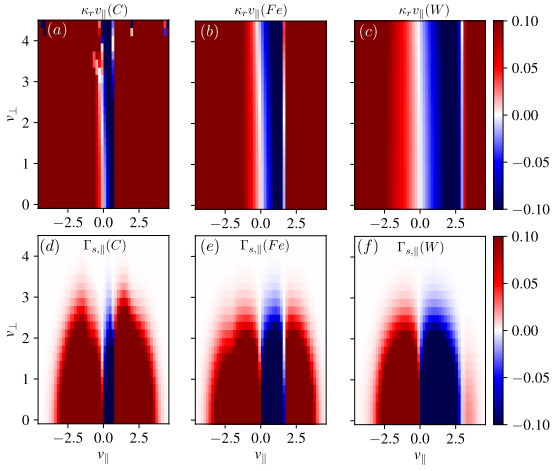

Figure 4. $\kappa_r v_\parallel$ (top) and the parallel compressibility pinch $\Gamma_{s,\parallel}\left(\kappa_r v_\parallel\right)$ (bottom) in $\left(v_\parallel, v_\perp\right)$ plane for carbon (left), iron (center) and tungsten (right) ions at $z = 1.2$. Results are shown for $k_y\rho_D = 0.3$ with $\hat{s} = -0.9$.

$\Gamma_{s,\perp}$ are enhanced with increasing $\hat{s}$, so $\langle\Gamma_{s,\parallel}\rangle$ increases slightly with respect to $\langle\Gamma_{s,\perp}\rangle$. While for $\hat{s} < 0$, $\Gamma_{s,\parallel}$ is enhanced and $\Gamma_{s,\perp}$ is reduced with decreasing $\hat{s}$, resulting in $\langle\Gamma_{s,\parallel}\rangle$ being strongly enhanced with respect to $\langle\Gamma_{s,\perp}\rangle$. Due to the combination of these separate effects of $\hat{s}$ on $\Gamma_{s,\parallel}$ and $\Gamma_{s,\perp}$, we observe the tendency of $\langle\Gamma_{s,\parallel}\rangle / |\langle\Gamma_{s,\perp}\rangle|$ when varying $\hat{s}$ shown in Fig. 1. The key question is: why $\Gamma_{s,\parallel}$ is enhanced when the gradient of turbulence intensity becomes large ?

Parallel frequency reversal.–Based on Eq. (2), $\Gamma_{s,\parallel}$ is proportional to the parallel frequency $\kappa_r v_\parallel$. Fig.4 shows the structure of $\kappa_r v_\parallel$ (top) and $\Gamma_{s,\parallel}\left(\kappa_r v_\parallel\right)$ (bottom) of different heavy ions in $\left(v_\parallel, v_\perp\right)$ plan at $z = 1.2$ in the simulation with $\hat{s} = -0.9$. In tungsten case, $\kappa_r v_\parallel$ (Fig.4c) is generally negative (positive) in positive (negative) velocity region and symmetric with respect to $v_\parallel = 0$, which seems to be consistent with the conventional description with $k_\parallel v_\parallel$. Therefore an outward $\Gamma_{s,\parallel}$ is produced in the negative velocity zone, meanwhile an inward $\Gamma_{s,\parallel}$ is produced in the positive velocity zone, as shown in Fig. 4f. The total $\Gamma_{s,\parallel}$ is not very large, as $\Gamma_{s,\parallel}\left(v_\parallel > 0\right)$ tends to cancel $\Gamma_{s,\parallel}\left(v_\parallel < 0\right)$.

It shall be noticed that in Fig.4c the parallel drift frequency of tungsten ions reverses the sign to positive in high velocity zone with $v_\parallel \geq 2.9$. However as the equilibrium is Maxwellian F_{sM} and $F_{sM}\left(v_\parallel \geq 2.9\right) \sim 0$, the frequency reversal in high velocity zone only has a little contribution to tungsten flux, as shown in Fig. 4f. In iron case, $\kappa_r v_\parallel$ seems to follow the conventional description in low velocity zone with $|v_\parallel| < 1.6$, but reverses the sign to positive in the zone of $v_\parallel \geq 1.6$(Fig.4b), and a non-negligible positive flux is produced(Fig.4e). In carbon case, $\kappa_r v_\parallel$ reverses the sign at around $v_\parallel \geq 0.73$(Fig.4a), and the contribution to the transport flux is significant,

since the parallel compressibility pinch $\Gamma_{s,\parallel}$, which is directed inward and dominates in the positive velocity zone in tungsten case, becomes outward in carbon case, as compared in Fig. 4d and Fig. 4f. This qualitative difference strongly enhances the parallel compressibility pinch of carbon ions.

Phase and Amplitude effect.–Here we explain the parallel frequency reversal by directly resolving the heavy ion parallel drift frequency. Since the mass and the charge of heavy ions are much larger than those of the bulk plasma, i.e., $m_s/m_D \gg 1$ and $e_s/e \gg 1$, the gyrokinetic equation of heavy ions is expanded in terms of the zeroth order $\mathcal{L}_0 \sim -i\omega$, the first order $\mathcal{L}_1 \equiv v_\parallel \nabla_\parallel$ and the second order $\mathcal{L}_2 \sim i\boldsymbol{k}_\perp \cdot \boldsymbol{v}_{sd}$ operators[20], with which, we can write: $(\mathcal{L}_0+\mathcal{L}_1+\mathcal{L}_2)\, g_{s\boldsymbol{k}_\perp} = \mathcal{L}_0 \frac{e_s F_{sM} J_{0s}\phi_{\boldsymbol{k}_\perp}}{T_s}$. Expanding $g_{s\boldsymbol{k}_\perp}$ into $g_{s\boldsymbol{k}_\perp,0}$, $g_{s\boldsymbol{k}_\perp,1}$, ..., etc, we find $g_{s\boldsymbol{k}_\perp,0} = \frac{q_s F_{sM} J_{0s}\phi_{\boldsymbol{k}_\perp}}{T_s}$, $g_{s\boldsymbol{k}_\perp,1} = -\frac{v_\parallel \nabla_\parallel g_{s\boldsymbol{k}_\perp,0}}{(-i\omega_r+\gamma)}$, and $g_{s\boldsymbol{k}_\perp,n} = -\frac{i\omega_{sd} g_{s\boldsymbol{k}_\perp,n-2}+v_\parallel \nabla_\parallel g_{s\boldsymbol{k}_\perp,n-1}}{(-i\omega_r+\gamma)}$. Here we only solve κ up to the first order. Using $g_{s\boldsymbol{k}_\perp,0}$ and $g_{s\boldsymbol{k}_\perp,1}$, we find

$$i\kappa = \nabla_\parallel \ln\left(J_{0s}\phi_{\boldsymbol{k}_\perp}\right) + \nabla_\parallel \left[v_\parallel \nabla_\parallel \ln\left(J_{0s}\phi_{\boldsymbol{k}_\perp}\right)\right]/i\omega + \ldots\,, \tag{3}$$

and the parallel frequency $\kappa_r v_\parallel$ is:

$$\kappa_r v_\parallel \simeq v_\parallel \nabla_\parallel \theta_{\boldsymbol{k}_\perp} + \frac{-\omega_r v_\parallel^2 \nabla_\parallel^2 \ln|\phi_{\boldsymbol{k}_\perp}|}{(\omega_r^2+\gamma^2)}\,, \tag{4}$$

where $\theta_{\boldsymbol{k}_\perp}(z)$ and $|\phi_{\boldsymbol{k}_\perp}(z)|$ are respectively the phase and the amplitude of $\phi_{\boldsymbol{k}_\perp}(z)$, defined as $\phi_{\boldsymbol{k}_\perp} = |\phi_{\boldsymbol{k}_\perp}| e^{i\theta_{\boldsymbol{k}_\perp}}$. As $v_\parallel$ is a function of z in an inhomogeneous magnetic field, one can not simply take $v_\parallel$ outside the $\nabla_\parallel$ operator. A term proportional to the mirror force $\mu\nabla_\parallel B$ is neglected in Eq.(4), since $\nabla_\parallel B$ is proportional to the inverse aspect ratio parameter $\epsilon\,(=0.105)$, which is small in a large aspect ratio tokamak. Hence up to the first order, $\kappa_r v_\parallel$ is nearly independent of the perpendicular velocity coordinates, which is consistent with the numerical results shown in Fig.4.

Based on Eq.(4), in the lowest order $\kappa_r v_\parallel$ is determined only by the profile of the phase of the electrostatic potential, meaning that particles with positive and negative parallel velocity shall have opposite parallel frequency, e.g., the conventional theory may still work in the lowest order. If $\phi_{\boldsymbol{k}_\perp}(z)$ satisfies $\phi_{\boldsymbol{k}_\perp} = |\phi_{\boldsymbol{k}_\perp 0}| e^{ik_\parallel z}$, $\nabla_\parallel \theta_{\boldsymbol{k}_\perp}$ gives $k_\parallel$, hence the conventional solution is actually the phase effect of the turbulence on the plasma parallel structure in a ideal case, i.e., $\theta_{\boldsymbol{k}_\perp}(z) = k_\parallel z$. The second term is determined by the profile of the turbulence intensity along z direction, it is the amplitude effect of the turbulence on the plasma parallel structure, which becomes significant when the gradient of the turbulence intensity becomes large along the magnetic field line. Moreover it depends explicitly on the parallel velocity $v_\parallel$, and hence

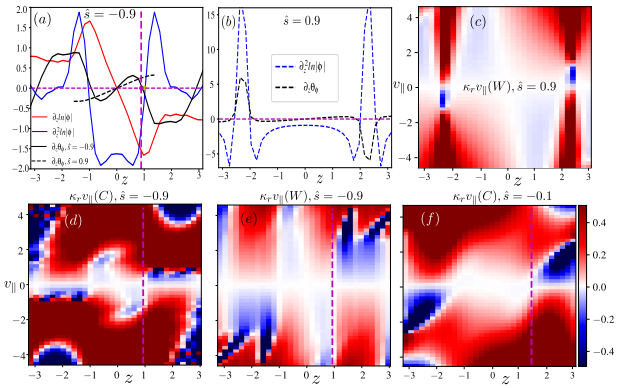

Figure 5. (a): $\partial_z\theta_{\mathrm{k}_\perp}$, $\partial_z \ln|\phi_{\mathrm{k}_\perp}|$ and $\partial_z^2 \ln|\phi_{\mathrm{k}_\perp}|$ as a function of z in the case with $\hat{s}=-0.9$. Black dashed curve shows $\partial_z\theta_{\mathrm{k}_\perp}$ with $\hat{s}=0.9$. The green, magenta and yellow points mark respectively the positions where v_{sd}, $\partial_z\theta_{\mathrm{k}_\perp}$ and $\partial_z^2\ln|\phi_{\mathrm{k}_\perp}|$ reverse the sign. (b): $\partial_z\theta_{\mathrm{k}_\perp}$ and $\partial_z^2\ln|\phi_{\mathrm{k}_\perp}|$ in the case with $\hat{s}=0.9$. (c) and (e) show respectively $\kappa_r v_\parallel$ of tungsten in $(v_\parallel, z)$ plane with $\hat{s}=0.9$ and $\hat{s}=-0.9$. (d) and (f) show $\kappa_r v_\parallel$ of carbon with $\hat{s}=-0.9$ and $\hat{s}=-0.1$. The vertical magenta lines in (a), (d), (e) and (f) mark the position where $\partial_z\theta_{\mathrm{k}_\perp}=0$. Results are shown for $k_y\rho_D=0.3$ mode.

can reverse the sign of the parallel frequency if $v_\parallel$ is large enough. Note that the amplitude effect of the turbulence on the ion parallel structure is reported here for the first time in kinetic plasma turbulence.

Fig.5a shows the profile of $\partial_z\theta_{\boldsymbol{k}_\perp}$, $\partial_z\ln|\phi_{\boldsymbol{k}_\perp}|$and $\partial_z^2\ln|\phi_{\boldsymbol{k}_\perp}|$ along z direction with $\hat{s}=-0.9$. $\partial_z\theta_{\boldsymbol{k}_\perp}$, $\partial_z^2\ln|\phi_{\boldsymbol{k}_\perp}|$ and the magnetic drift velocity $\mathbf{v}_{sd}$ reverse the sign almost in the same position, as marked by the magenta, yellow and green circles, respectively. When $\partial_z\theta_{\boldsymbol{k}_\perp}$ is close to zero(marked by the magenta vertical lines in Fig.5d and Fig.5e), $\kappa_r v_\parallel$ starts to reverse the sign, since the second term plays a role. The frequency reversal occurs in low velocity zone and exists in a long region in z direction ($z>1.0$,$v_\parallel \gtrsim 0.7$) in carbon case (Fig.5d). However with a weak magnetic shear, the gradient of turbulence intensity is small, the frequency reversal also occurs, but in relatively high velocity zone in carbon case, as shown in Fig.5f with $\hat{s}=-0.1$.

The frequency reversal is also observed in tungsten case with $\hat{s}=-0.9$, but occurs in high velocity zone and exists only in a narrow region along z (Fig.5e). Fig.5b shows $\partial_z\theta_{\boldsymbol{k}_\perp}$ and $\partial_z^2\ln|\phi_{\boldsymbol{k}_\perp}|$ with $\hat{s}=0.9$. $\partial_z^2\ln|\phi_{\boldsymbol{k}_\perp}|$ becomes much larger, while $\partial_z\theta_{\boldsymbol{k}_\perp}$is roughly in the same order or even smaller compared to that with $\hat{s}=-0.9$, as shown in Fig.5a, hence the kinetic effect is much stronger. Even for tungsten, the parallel frequency can reverse sign in low velocity zone (Fig.5c), and the parallel compressibility pinch is enhanced. Finally $\langle\Gamma_{s,\parallel}\rangle / |\langle\Gamma_{s,\perp}\rangle|$ increases, even though $\Gamma_{s,\perp}$ is very strong with a large positive magnetic shear. The result in Fig. 1 is shown for $k_y\rho_D=0.3$ mode. Due to the $1/k_y$ dependence in $\langle\Gamma_{s,\parallel}\rangle / |\langle\Gamma_{s,\perp}\rangle|$[20], the outward flux of $k_y\rho_D=0.1$ mode

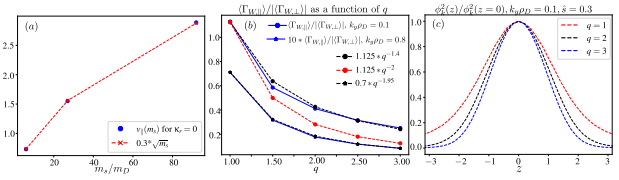

Figure 6. Left figures shows $v_\parallel$ ($\kappa_r = 0$) as a function of the mass m_s at $z = 1.17$ with $\hat{s} = -0.9$. Center figure presents $\langle\Gamma_{W,\parallel}\rangle / |\langle\Gamma_{W,\perp}\rangle|$(blue solid) as a function of the safety factor q for $k_y\rho_D = 0.1$ and $k_y\rho_D = 0.8$ modes, here $\hat{s} = 0.3$. Dashed curves are used to fit the numerical results. Right figure presents $\phi^2_{k_\perp}/\phi^2_{k_\perp}$ ($z = 0$) along the magnetic field line with different safety factor.

is much stronger and $\Gamma_{s,\parallel}$ nearly exceeds $\Gamma_{s,\perp}$, even for tungsten ions (with $\hat{s} = 1.3$, $\langle\Gamma_{W,\parallel}\rangle / |\langle\Gamma_{W,\perp}\rangle|$=0.8). Based on the tendency, $\Gamma_{s,\parallel}$ could be further enhanced with stronger positive $\hat{s}$, meaning that in a proper parameter range it shall be possible to reverse the pinch direction from inward to outward with a large enough positive magnetic shear.

As $v_\parallel$ is normalized by the thermal speed $\sqrt{T_s/m_s}$, from Eq. (4) we predict that

$$v_\parallel\,(\kappa_r = 0) \propto \sqrt{m_s}\ , \tag{5}$$

e.g., the $v_\parallel$ where the parallel frequency reverses the sign in velocity space is proportional to $\sqrt{m_s}$. This is well confirmed by the simulation data, as shown in Fig. 6a, where $v_\parallel$ at which different ions reverse the parallel frequency clearly follows a $\sqrt{m}$ scaling.

To further test the validity of above results, we fix $\hat{s} = 0.3$, but varies the safety factor q. Note that in previous case with $\hat{s} = 0.3$ and $q = 1.29$, the amplitude effect is not obvious. Based on the lowest order solution, $\langle\Gamma_{W,\parallel}\rangle / |\langle\Gamma_{W,\perp}\rangle|$ shall follow a $1/q^2$ scaling, as $v_\parallel\nabla_\parallel\left(v_\parallel\nabla_\parallel\right) \sim 1/q^2$. However, Fig.6c shows that the parallel gradient of the turbulence intensity is enhanced with increasing q in present case, one may think that $\Gamma_{W,\parallel}$ may be enhanced with a high q. Indeed, $\langle\Gamma_{W,\parallel}\rangle / |\langle\Gamma_{W,\perp}\rangle|$ follows a $1/q^{1.4}$($1/q^{1.2}$ for carbon) scaling for $k_y\rho_D = 0.1$ mode in Fig.6b. For high k_y modes with much higher turbulence frequency, the amplitude effect is mitigated and $\langle\Gamma_{W,\parallel}\rangle / |\langle\Gamma_{W,\perp}\rangle|$ is close to $1/q^2$. From this result, one shall find that various parameters, not only the magnetic shear can modify the turbulence profile along the magnetic field line, which is well-known in plasma turbulence. So the parallel frequency reversal due to the amplitude effect of turbulence can be triggered by various parameters in various plasmas.

Before the end, we shall mention that in Fig.2b, the reversal of the parallel frequency seems to enhance the part of the outward flux in the perpendicular compressibility pinch. With $\hat{s} = -0.9$, the ratio of the outward flux to the inward flux in $\Gamma_{s,\perp}$ is roughly 35% for carbon ions. For tungsten, this ratio is 10%. It displays that the outward pinch in $\Gamma_{s,\perp}$ changed by the parallel frequency reversal is nearly in a comparable level compared to the inward pinch, at least for carbon ions. In a proper parameter range with strong enough negative magnetic shear, the outward flux in $\Gamma_{s,\perp}$ may be further enhanced due to the parallel frequency reversal. This is especially interesting in ITG case and needs to be investigate. In fact, as the parallel frequency appears in various parts in the transport equation, the parallel frequency reversal shall modify many transport results.

Summary.–We report the reversal of the parallel drift frequency when the gradient of the turbulence intensity becomes large along the magnetic field line. As a result, the ion fluxes related to the parallel dynamics are seen to be strongly enhanced, rather than reduced or suppressed, which is a novel phenomenon in kinetic plasma.

The heavy ion parallel frequency, i.e., $\kappa_r v_\parallel$ rather than $k_\parallel v_\parallel$, is derived for the first time in the gyrokinetic framework, which is the sum of the phase effect ($\sim v_\parallel\nabla_\parallel\theta_\phi$) and the amplitude effect ($\sim v_\parallel^2\nabla_\parallel^2\ln|\phi|/\omega_r$). The former one gives an opposite frequency for particles with $v_\parallel$ and $-v_\parallel$, and tends to reduce the transport. The later one gives the same frequency for $v_\parallel$ and $-v_\parallel$ particles and tends to enhance the transport. The ion flux related to the parallel dynamics is a competition of these two and co-determined by the ion mass, the turbulence frequency and the (phase and amplitude) profile of the turbulence.

We emphasize that the parallel frequency reversal can be triggered by various parameters in various plasmas, not only the magnetic shear and the safety factor shown here. Moreover the amplitude effect depends on the turbulence frequency, the parallel frequency reversal should be different in ITG case and needs to be investigated. It is also noteworthy that the second order solution shall be considered if $\omega_{sd} \lesssim v_\parallel\nabla_\parallel$, where we shall see some $v_\parallel^3$ terms and the magnetic structure appearing in the ion parallel frequency. Last, we can check the parallel structure of electrons and deuterium ions with the method here, but the mechanism is more complicated. We leave these for the future work.

This work is supported by MEXT as "Program for Promoting Researches on the Supercomputer Fugaku" (Exploration of burning plasma confinement physics, hp200127, hp210178, hp220165 and JPMXP1020200103).

[1] Z. Lin, T. S. Hahm, W. W. Lee, W. M. Tang, and R. B. White, Science New Series, **281**, pp. 1835 (1998).
[2] T. Görler and F. Jenko, Physics of Plasmas **15**, 102508 (2008).

[3] X. Garbet, Y. Idomura, L. Villard, and T. Watanabe, Nuclear Fusion **50**, 043002 (2010).

[4] S. Maeyama, Y. Idomura, T.-H. Watanabe, M. Nakata, M. Yagi, N. Miyato, A. Ishizawa, and M. Nunami, Phys. Rev. Lett. **114**, 255002 (2015).

[5] S. Maeyama, T.-H. Watanabe, M. Nakata, M. Nunami, Y. Asahi, and A. Ishizawa, Nature Communications **13**, 3166 (2022).

[6] J. Citrin, C. Bourdelle, P. Cottier, D. F. Escande, Ö. D. Gürcan, D. R. Hatch, G. M. D. Hogeweij, F. Jenko, and M. J. Pueschel, Physics of Plasmas **19**, 062305 (2012).

[7] J. Candy and R. E. Waltz, Journal of Computational Physics **186**, 545 (2003).

[8] X. Garbet, L. Garzotti, P. Mantica, H. Nordman, M. Valovic, H. Weisen, and C. Angioni, Phys. Rev. Lett. **91**, 035001 (2003).

[9] C. Angioni and A. G. Peeters, Phys. Rev. Lett. **96**, 095003 (2006).

[10] C. Bourdelle, X. Garbet, F. Imbeaux, A. Casati, N. Dubuit, R. Guirlet, and T. Parisot, Phys. Plasmas **14**, 112501 (2007).

[11] S. Futatani, X. Garbet, S. Benkadda, and N. Dubuit, Phys. Rev. Lett. **104**, 015003 (2010).

[12] C. Angioni, Plasma Physics and Controlled Fusion **63**, 073001 (2021).

[13] T.-H. Watanabe, S. Maeyama, and M. Nakata, Nuclear Fusion **63**, 054001 (2023).

[14] T.-H. Watanabe and H. Sugama, Nuclear Fusion **46**, 24 (2005).

[15] E. J. Strait, L. L. Lao, M. E. Mauel, B. W. Rice, T. S. Taylor, K. H. Burrell, M. S. Chu, E. A. Lazarus, T. H. Osborne, S. J. Thompson, and A. D. Turnbull, Phys. Rev. Lett. **75**, 4421 (1995).

[16] F. M. Levinton, M. C. Zarnstorff, S. H. Batha, M. Bell, R. E. Bell, R. V. Budny, C. Bush, Z. Chang, E. Fredrickson, A. Janos, J. Manickam, A. Ramsey, S. A. Sabbagh, G. L. Schmidt, E. J. Synakowski, and G. Taylor, Phys. Rev. Lett. **75**, 4417 (1995).

[17] Kessel, Manickam, Rewoldt, and Tang, Physical review letters **72**, 1212 (1994).

[18] P. H. Rutherford and E. A. Frieman, The Physics of Fluids **11**, 569 (1968).

[19] E. A. Frieman and L. Chen, Physics of Fluids **25**, 502 (1982).

[20] S. Xu, S. Maeyama, and T.-H. Watanabe, Phys. Rev. Res. **4**, 043156 (2022).

[21] C. Angioni, R. Bilato, F. Casson, E. Fable, P. Mantica, T. Odstrcil, and M. Valisa, Nuclear Fusion **57**, 022009 (2016).

[22] T. Pütterich, R. Neu, R. Dux, A. Whiteford, M. O'Mullane, H. Summers, and the ASDEX Upgrade Teams, Nuclear Fusion **50**, 025012 (2010).

[23] S. Xu, S. Maeyama, and T.-H. Watanabe, Nuclear Fusion **62**, 064003 (2022).